

Special Section:

Exploration of the Activity of Asteroid (101955) Benu

Key Points:

- We simulate 355 years (1780–2135) of particle ejection from asteroid (101955) Benu
- Meteor flux (at Earth) of particles from Benu is $< 1/\text{yr}$ until 2100 AD, peaking in 2182 AD at 161 Bennuids
- The Benu particle stream encircles in 80 years, and 99% of stream members remain associable for all 420 years of the simulation

Correspondence to:R. E. Melikyan,
rmelikyan@lpl.arizona.edu**Citation:**

Melikyan, R. E., Clark, B. E., Hergenrother, C. W., Chesley, S. R., Nolan, M. C., Ye, Q.-Z., & Lauretta, D. S. (2021). Benu's natural sample delivery mechanism: Estimating the flux of Bennuid meteors at Earth. *Journal of Geophysical Research: Planets*, 126, e2020JE006817. <https://doi.org/10.1029/2020JE006817>

Received 28 DEC 2020





Accepted 4 AUG 2021

Author Contributions:**Conceptualization:** R. E. Melikyan, B. E. Clark, C. W. Hergenrother, Q.-Z. Ye**Data curation:** R. E. Melikyan, S. R. Chesley, D. S. Lauretta**Formal analysis:** R. E. Melikyan, B. E. Clark, S. R. Chesley, M. C. Nolan**Funding acquisition:** B. E. Clark, D. S. Lauretta**Investigation:** R. E. Melikyan, C. W. Hergenrother, S. R. Chesley, M. C. Nolan**Methodology:** R. E. Melikyan, B. E. Clark, C. W. Hergenrother, S. R. Chesley, M. C. Nolan, Q.-Z. Ye

© 2021. The Authors.

This is an open access article under the terms of the [Creative Commons Attribution License](#), which permits use, distribution and reproduction in any medium, provided the original work is properly cited.

Benu's Natural Sample Delivery Mechanism: Estimating the Flux of Bennuid Meteors at Earth

 R. E. Melikyan^{1,2} , B. E. Clark¹ , C. W. Hergenrother² , S. R. Chesley³ , M. C. Nolan² , Q.-Z. Ye⁴ , and D. S. Lauretta²
¹Department of Physics and Astronomy, Ithaca College, Ithaca, NY, USA, ²Lunar and Planetary Laboratory, University of Arizona, Tucson, AZ, USA, ³Jet Propulsion Laboratory, California Institute of Technology, Pasadena, CA, USA,

⁴Department of Astronomy, University of Maryland, College Park, MD, USA

Abstract NASA's OSIRIS-REx mission observed millimeter- to centimeter-scale pebbles being ejected from the surface of asteroid (101955) Benu, indicating that Benu is an active asteroid. About 30% of these particles escape from Benu, and the minimum orbital intersection distance (MOID) between Benu and Earth suggest the possibility of a “Bennuid” particle flux at Earth. We characterize the evolution of Benu's particle stream and potential for meteor flux by simulating weekly particle ejections between the years 1780 and 2135 continuing their dynamical evolution until 2200. Ejections are modeled as a discrete release of 95 particles every week. The meteoroid stream is found to be fully distributed around Benu's orbital path in 80 ± 40 years. Individual particles and streams remain associable to Benu for the entire 420 years simulated. Particle flux at Earth is predicted to begin in 2101, as the Benu-Earth MOID reaches minimum values. The year of highest particle flux, 2182, experiences 161 Earth intersections and accounts for $\sim 1/4$ of our predicted meteors. Our methods can be expanded to study the history and structure of the general meteoroid population and to estimate flux from specific near-Earth asteroids.

Plain Language Summary NASA's OSIRIS-REx asteroid sample return mission observed coin-sized rock fragments launching from the surface of the near-Earth asteroid Benu. Although many of these particles fall back down to the surface of Benu, about 30% escape the gravitational influence of this small celestial body and enter orbits around the Sun. By simulating the motion of small particles ejected from Benu over the years 1780–2200, we test whether they eventually encounter Earth's atmosphere. The predicted particle flux ranges from undetectable to ~ 1 meteor per 10 h, a rate which is comparable with the weakest known meteor showers. We find that ejected particles spread out along Benu's orbit and occupy positions around the entire circle within 80 years. For the 420 years simulated, the particles can be easily associated with Benu by the similarities in their orbits. Particles we simulated being ejected from Benu are not found to impact Earth until 2101. We predict a maximum flux in the year 2182, with around 161 intersecting meteors potentially visible as shooting stars. Our methods can be used to investigate the possibility of meteoroid streams from other near-Earth asteroids to identify sources of known meteoroid streams and meteor showers.

1. Introduction

The growing evidence for asteroid activity suggests that comets may not be the sole contributors of meteor flux at Earth. For example, active asteroid (3200) Phaethon has been identified as the parent body of the major Geminid meteor shower (Jenniskens, 2006). The near-Earth asteroid target of NASA's OSIRIS-REx asteroid sample return mission, (101955) Benu, exhibits meteoroid-generating activity (Hergenrother, Adam, et al., 2020; Hergenrother, Maleszewski, et al., 2020; Lauretta et al., 2019). With observed ejection events producing sometimes hundreds of centimeter-sized particles at velocities of up to a few meters per second, and a small minimum orbit intersection distance (MOID) with Earth (Chesley et al., 2020), it is reasonable to ask if meteoroids ejected from Benu could contribute to meteor activity at Earth.

The most probable mechanisms for activity at Benu are thermal fracturing, phyllosilicate dehydration, and impacts (Bottke et al., 2020; Lauretta et al., 2019; Molaro et al., 2020). Orbit determination analysis of the observed ejection events found that $\sim 30\%$ of particles escape from Benu on hyperbolic trajectories (Chesley

Project Administration: B. E. Clark, C. W. Hergenrother, D. S. Lauretta
Resources: R. E. Melikyan, B. E. Clark, C. W. Hergenrother, S. R. Chesley, Q.-Z. Ye, D. S. Lauretta
Software: R. E. Melikyan, S. R. Chesley, M. C. Nolan
Supervision: B. E. Clark, C. W. Hergenrother, S. R. Chesley, D. S. Lauretta
Validation: R. E. Melikyan, B. E. Clark, C. W. Hergenrother, S. R. Chesley, M. C. Nolan, Q.-Z. Ye
Visualization: R. E. Melikyan, B. E. Clark, S. R. Chesley
Writing – original draft: R. E. Melikyan
Writing – review & editing: R. E. Melikyan, B. E. Clark, C. W. Hergenrother, S. R. Chesley, M. C. Nolan, Q.-Z. Ye, D. S. Lauretta

et al., 2020; Hergenrother, Maleszewski, et al., 2020; Leonard et al., 2020). Chesley et al. (2020) and Leonard et al. (2020) investigated the trajectories of the ~70% of particles that remain bound to Bennu on orbital and suborbital paths. To complement these works, we developed an orbital integration model to predict the fate of the escaped hyperbolic particles.

With its low inclination (~ 6°), eccentricity (~ 0.2), and MOID (currently within 1.25 lunar distances), Bennu is a plausible candidate parent body for meteor activity at Earth. Bennu's recent and near-term future close approaches with Earth are shown in Figure 1. Each close approach affects how well we can predict Bennu's subsequent motion. Secular perturbations of Bennu's orbit are expected to further decrease the MOID over this upcoming century, reaching values within Earth's cross sectional radius between 2100 and 2250 (Chesley et al., 2014).

Two preceding studies examined the dynamical evolution of ejecta from Bennu (Kováčová et al., 2020; Ye, 2019). Ye (2019) presented initial estimations for peak meteor flux rates assuming cometary style production. Using the Emery et al. (2014) upper limit of dust flux, Ye (2019) suggested local meteor fluxes on the order of $10^{-6} \text{ km}^{-2} \text{ hr}^{-1}$ over the next several decades. These estimates, which ended in 2100, increase by an order of magnitude near the year 2080 which can be correlated with a major close approach (Figure 1) and the decreasing Bennu-Earth MOID (Chesley et al., 2014). Kováčová et al. (2020) provide a detailed analysis of a potential meteor stream of 5,000 produced particles ejected gradually along a Bennu-like orbit in the year 1600. From this stream, Kováčová et al. (2020) predict a radiant at Earth of ($\alpha = 3.3 \pm 2.1^\circ$, $\delta = -34.7 \pm 1.7^\circ$) and include a detailed analysis of the evolution of particle MOIDs, which differ from the parent body, with insights into the orbital spread of the resulting stream. The present study expands on these past works by numerically integrating nearly 1.8 million continuously produced particles during a time frame over which Bennu's position is precisely known (1780–2135) and constraining their initial conditions to the characteristics observed by the OSIRIS-REx mission.

Similar to cometary dust, particles ejected from Bennu are susceptible to planetary perturbations and are constantly subject to the effects of solar radiation. This radiation operates in the form of solar radiation pressure (SRP) and Poynting-Robertson (PR) drag (Burns et al., 1979). In contrast with cometary dust, meteoroids from Bennu are produced throughout its orbit (Hergenrother, Maleszewski, et al., 2020). Our orbital

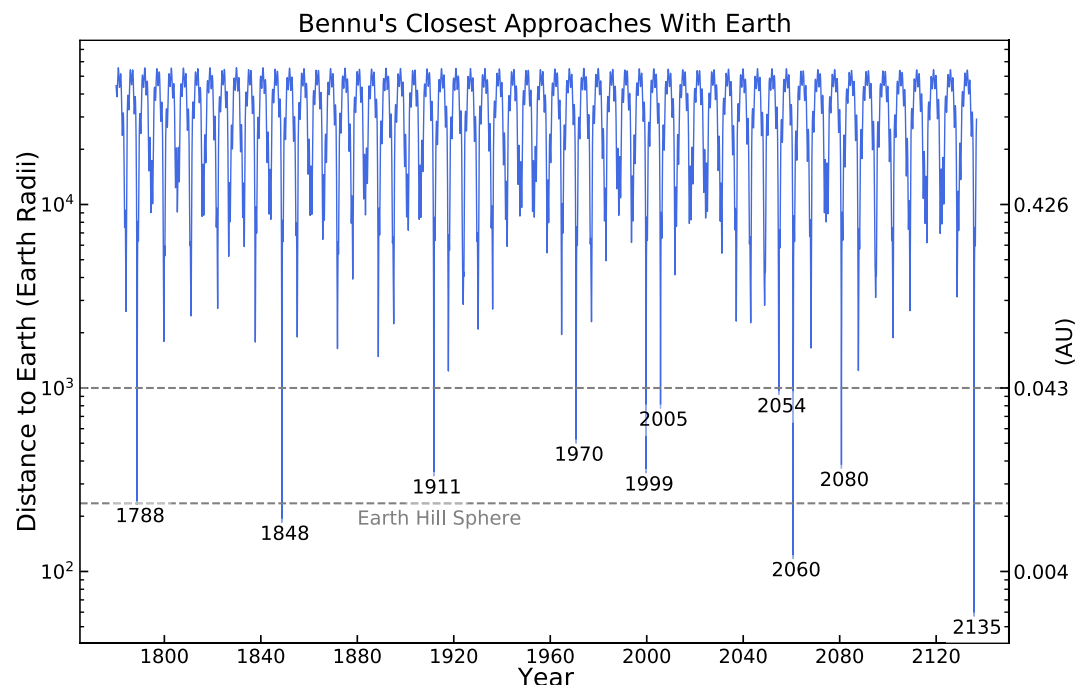


Figure 1. With a ~1.2-year orbital period, Bennu approaches close to Earth every 5–7 years. Its closest approaches are noted here for distances $\leq 1,000$ Earth Radii (or 0.043 AU).

integrations simulate the motion and evolution of Bennu's particles under assumptions of productivity about the entirety of Bennu's orbit. Activity at comets occur around their perihelion passages, as the body enters a range close enough for volatiles to react to the Sun's energy. Particle production events at Bennu are observed to occur regardless of orbital position.

Owing to uncertainties in Bennu's orbit before 1780 and after 2135, we constrain meteoroid stream production to this time range (355 years), though our simulations propagate the motion of the resultant stream out to 2200, for a total of 420 years simulated. These constraints are necessary because we do not know where Bennu was with sufficient accuracy before 1780 (see Table 8 of Chesley et al., 2014). Particles released before 1780 certainly could reach Earth, but the trajectories of such particles are difficult to characterize because of the large uncertainties in the position of Bennu at the time of ejection. We analyze the output from the integrations for the peak meteor intersection flux at Earth for each year in the simulation. We contextualize these impact rates through analysis and characterization of the stream by:

1. Investigating the timescale of stream encircling (defined in Section 2.3)
2. Determining timescales of associability to the parent body
3. Analyzing initial conditions that may affect impact probabilities

Our results offer information about the long-term trajectories of the particles that have been observed leaving Bennu and provide testable projections for ground-based "Bennuid" meteor observations.

2. Particle Dynamics

There are two aspects that allow ejected particles to follow Earth-crossing orbits while Bennu does not: their ejection velocities and their susceptibility to SRP and PR drag forces. The resulting particle stream can be characterized by encircling of particle orbits and their associability to the parent body (Ye, Brown, & Pokorný, 2016).

2.1. Observations of Ejection Velocities

By analyzing off-limb images (Bos et al., 2020) of Bennu taken by the on-board navigation camera NavCam 1, Chesley et al. (2020), Hergenrother, Maleszewski, et al. (2020), and Lauretta et al. (2019) found that particles ejected from Bennu range from millimeters to centimeters in diameter. In the photometry study by Hergenrother, Maleszewski, et al. (2020), the particle size distribution was found to range from NavCam 1's lower limit of detection at 1 mm (or smaller) to 7 cm, with the peak centered between 0.1 and 2.5 cm (Figure 2). These observed values are consistent with size distributions predicted for thermal fracturing (Molaro et al., 2020) and meteoroid impacts (Bottke et al., 2020). Observed ejection speeds of escaping particles range from a lower limit equal to Bennu's escape velocity $\sim 0.2 \text{ m s}^{-1}$ up to 3.26 m s^{-1} during the most energetic events (Hergenrother, Maleszewski, et al., 2020). Weighting the observed ejection velocities with the observed size distribution leads to a range of $0.2\text{--}1 \text{ m s}^{-1}$ for the speeds of the escaping population (Hergenrother, Maleszewski, et al., 2020). Based on meteorite analogs (Hamilton et al., 2019), Hergenrother, Maleszewski, et al. (2020) assume a particle bulk density of about $2,000 \pm 500 \text{ kg m}^{-3}$, and estimate particle production rates of $\sim 10 \text{ kg}$ per Bennu orbit.

Observations of the particle ejections show that particles are released most often during Bennu's local afternoon and evening (Hergenrother, Adam, et al., 2020). Though the energy added or removed from the particles' orbits due to ejection velocity is small compared to heliocentric motion, small differences in initial conditions can lead to large effects, especially for bodies like Bennu that have close encounters with major perturbers, such as Earth. A range in ejection velocities causes particles to either pull ahead or lag behind Bennu in its heliocentric orbit, affecting the timing of future close interactions with Earth and contributing to the formation of a particle stream.

2.2. Particle Stream Coherence

Because their ejection velocities are much smaller than Bennu's orbital velocity, the orbits of the ejected particles will remain characteristically similar to their parent body. A commonly used parameter for quantifying

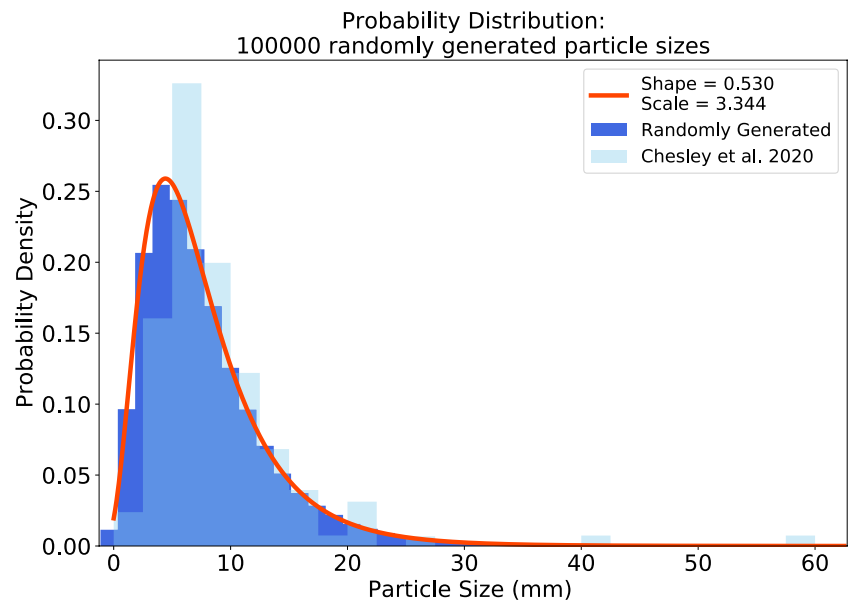


Figure 2. The particle size distribution reported by Chesley et al. (2020) is fit with a log-normal distribution. The range of 1–25 mm is broken into 24 equally sized bins and follows the distribution of the fitted curve. The randomly generated particle bins represents the values used in our model.

Keplerian orbital similarity is the D_{sh} criterion, which evaluates distances in orbital element space (a , e , i , ω , and Ω ; Jenniskens, 2006; Southworth & Hawkins, 1963). Two orbits are considered associable if their D_{sh} criterion is less than 0.15. Due to chaotic gravitational perturbations, particles on Bennu-like orbits, on average, remain associable on the order of 7,000 years. Such similarity; however, is crucial in this study as it is a necessary factor in confirming if any observed meteor flux is related to Bennu. To be recognized as meteors from Bennu, ejected particles must be on orbits similar enough to Bennu that they are recognized as Bennuids as they approach Earth, but different enough that their orbits intersect with Earth whereas Bennu's does not.

2.3. Importance of Solar Radiation Forces on the Particle Stream

For particles in the observed centimeter-size range, SRP and PR drag play a major role in their orbital evolution (Burns et al., 1979; Chesley et al., 2020; Ye, Hui, et al., 2016). Additional effects such as the momentary reduction of PR due to shadowing, or solar tides, as included in McMahon et al. (2020) are not considered due to their negligible contribution to the statistics of our particle population. We used a log-normal distribution which qualitatively matches the observed particle size distribution shown in Figure 2. For particles in the reported size range, the force caused by solar photon collisions ranges from 2×10^{-5} to 6×10^{-4} times the force of gravity. For SRP, the interaction is along the vector radial to the luminous body, in our case the Sun, which allows us to think of the force as a reduction of perceived gravitational influence from the central body. However, PR drag is a retarding force on the motion for orbiting bodies within and below the centimeter-size range. Owing to the effective mass loss of re-radiated photons biased in the direction of the particle motion, PR tends to decrease the semi-major axis (a) of bodies under its influence (Burns et al., 1979).

The combination of initial ejection velocity and the solar-induced non-gravitational forces enables a third difference between a parent body and its particles: the evolution of a particle stream about the parent body's orbit. Slight differences in their initial conditions allow the particles to quickly drift away relative to their parent body. In the limit of large numbers, cometary ejecta are fully distributed around their parent's orbit (encircled) within 200 years, and in some cases as quickly as 30 years (Ye et al., 2018). Encircling means a ring-shaped stream of dispersed ejecta along the circumference of the parent orbit. The density of this cloud of particles tends to uniformity along the orbital path as the standard deviation of the particle mean anomaly (M) surpasses 60° , where $\sigma M \geq 60$ implies that 99.7% of particles are distributed within the region of $\pm 180^\circ$ mean anomaly (Ye et al., 2018).

For example, the Leonids are an encircled meteoroid stream that produces an annual shower at Earth. This is caused by Earth crossing through comet 55P/Tempel-Tuttle's ejected debris. 55P has an orbital period of more than 33 years and yet we encounter its ejecta every year as we pass near the point of MOID between Earth and 55P. That MOID is ~ 3 lunar distances, whereas the Bennu-Earth MOID is only 1.25 lunar distances and decreasing over time. One might expect, therefore, that Bennu could also deliver an annual meteor shower. Vaubaillon et al. (2005) modeled the evolution of the Leonid dust stream to predict annual meteor flux densities which matched observations. We follow the computational methods of Vaubaillon's model: simulating the production and orbital evolution of many thousands of particles over the time range 1780–2200.

3. The Dynamical Environment

To model the dynamical evolution of the hyperbolic ejecta observed from active asteroid Bennu, we used the robust, freely available, N-body integrator package REBOUND (Rein & Liu, 2012). Our dynamical model is built to optimize accuracy of the particle stream evolution, for the investigation of dynamical behavior, lifetime of association, and predicted particle flux at Earth. We use the IAS-15 integrator which is a fifteenth-order, adaptive time-stepping, non-symplectic integrator that maintains integration error below machine precision for more than a billion orbits (Rein & Spiegel, 2015).

3.1. Simulation Development With Rebound

Chesley et al. (2014) found that regular close approaches to Earth limit the range of Bennu positional certainty to between 1780 and 2135. Planetary positions are well constrained well past this however, so our model remains accurate through the year 2200. Our first step in building an accurate simulation environment was to ensure that the massive bodies of the solar system maintained correct historically accepted positions throughout the modeled time frame. The bodies included, in addition to the Sun, are the eight planet, along with Pluto, Ceres, Pallas, Vesta, and Earth's Moon, with their respective masses matching those used in Jet Propulsion Laboratory (JPL)'s latest, most consistent, digital ephemeris, DE431 (Folkner et al., 2014), provided by NASA's Jet Propulsion Laboratory. These bodies constitute more than 99.98% of the mass relevant to this region of the solar system (Folkner et al., 2014).

Bennu and all generated ejecta are treated as mass-less particles. This is a reasonable assumption because our simulated particles are introduced with ejection velocities that account for Bennu's sphere of influence. We used Bennu's weekly state ephemeris, which matched that used by Chesley et al. (2014), to initiate particles at known Bennu locations. (Note: An alternative approach would be to integrate Bennu into the simulation and use its state to initialize new ejecta). A side effect of using the Bennu ephemeris is the inclusion of non-gravitational forces that are pertinent to Bennu's orbital evolution but are negligible for the ejecta. One such force is the Yarkovsky effect, which plays a strong role in the dynamical evolution of bodies of diameter 10^2 – 10^4 m over this timescale (Chesley et al., 2014). Hence, our simulations indirectly incorporate the Yarkovsky effect on Bennu while saving the computational expense of an additional non-gravitational force.

Particles have been observed ejecting from Bennu throughout its orbit (Hergenrother, Maleszewski, et al., 2020), and on average, ejections occur roughly several times per month. In our model, simulated particles are introduced weekly at known Bennu locations with randomized ejection velocities. These ejection velocities are included by projecting randomized velocities within the range 0.2 – 1 m s⁻¹ (representative of majority of observed ejecta speeds) onto a sphere and adding the resulting vector to the particles' initial state. This implementation was also used by Kováčová et al. (2020).

3.2. Implementation of Non-Gravitational Forces

Particles in the centimeter-sized particle regime are easily influenced by SRP and PR drag (Burns et al., 1979). We used REBOUNDx (Tamayo et al., 2020), which can incorporate computationally complex procedures into a REBOUND simulation environment without sacrificing computational speed. We included the solar effects, as defined by Burns et al. (1979), via the Radiation Forces package (Tamayo et al., 2020). The magnitude of this radiative effect depends on a parameter β corresponding to a radii generated according to

Table 1
Solar System Shift Deltas

Body	ΔR (m)	ΔR (m)	$\Delta \dot{R}$ (mm/s)	$\Delta \dot{R}$ (mm/s)
	Mean	Max	Mean	Max
Venus	85.32	86.97	0.28	0.29
Earth	32.27	36.35	0.11	0.12
Moon	321	485	1.27	1.82
Mars	9.3	11.9	0.03	0.04
Jupiter	0.2	0.4	0.0007	0.0009

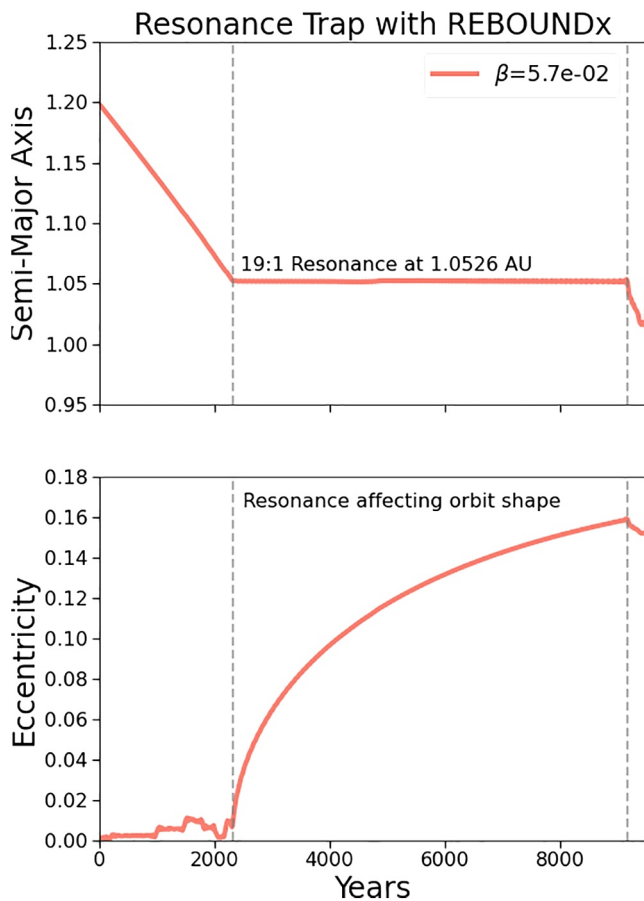


Figure 3. This figure shows a Sun, Earth, and particle three-body system, with expected orbital evolution of the particle under the effects of gravitational perturbations, solar radiation pressure (SRP), and Poynting-Robertson (PR) drag (Weidenschilling & Jackson, 1993). The sample particle (in this example, $\beta = 0.057$) will experience a constant decay in its orbit until caught in resonance with Earth. Once trapped, as noted by the first vertical line, the eccentricity of the orbit will continuously rise, until the resonance can no longer support the orbit shape, as noted by the second vertical line. This behavior was reproduced from Weidenschilling and Jackson (1993), using a REBOUND simulation with the REBOUNDx implementation of the radiation forces, giving us confidence in the accuracy of the simulated environment.

the observed size frequency distribution (Figure 2), which is assigned to each particle during initialization. β is the ratio of SRP relative to the solar gravitational force and can be obtained from

$$\beta = 1.148 \cdot 10^{-3} \frac{Q_{pr}}{\rho d}, \quad (1)$$

where Q_{pr} is the grain scattering efficiency, ρ is the particle density in kg m^{-3} , and d is the particle diameter in meters (values provided in Table 2; Jenniskens, 2006). β ranges from 2×10^{-5} to 6×10^{-4} for the particles in our simulations.

Other non-gravitational forces such as relativistic effects, solar wind drag, and mass shedding are assumed to be negligible for this study (Vaubaillon et al., 2005).

3.3. Assessing Simulation Accuracy

Because our objective is to create a simulated environment that is representative of the actual conditions that Bennu's particle stream experiences, we took additional measures to ensure accuracy. Each week, just before the introduction of a new particle, we correct the positions of the major bodies to match those reported by Folkner et al. (2014) in JPL's most recent solar system solution DE431. Our integrator was already highly accurate such that the weekly corrections are on the order of only 10 m for the inner planets and 1 m for the outer planets. These corrections are effective in the long run, as Earth's positional differences between internally integrated planets and the JPL solution could be as large as 2 Earth radii by the end of the 420-year period. The most significant rationale for this step in our integration method is to ensure the accuracy of the Moon's position, because the Moon's orbit is notoriously difficult to model effectively due to non-rigid-body motions of tides, etc. A summary of the position and velocity corrections (expressed as deltas) applied during this process is provided in Table 1.

We added one more test to ensure accuracy. A study by Weidenschilling and Jackson (1993) explores the effect of SRP and PR drag on orbital resonance traps. With our model, we were able to recreate a three-body resonance system that is detailed in their study (Figure 3). As expected, a particle under a constant transverse drag along its orbit will experience a drift toward the system's center. This drift is interrupted by the resonance trap, which will remain stable until the eccentricity reaches a critical value, above which it exits the trap.

Table 2

Parameters of Model

Production range	1780–2135
Full time range	1780–2200
Production rate	95 Particles/Week
Ejection speeds	0.2–1 (m s ⁻¹)
Particle diameters (<i>d</i>)	0.1–2.5 (cm)
Particle density (ρ)	2,000 (kg m ⁻³)
Scattering efficiency (Q_{pr})	1 ^a

^aBurns et al., 1979.

4. Simulation and Experimental Procedures

Our simulations model the evolution of Bennu's particle stream throughout the period when Bennu's orbit is best constrained (1780–2135). The integrations are extended through 2200 to better understand the future of the particle stream. The ejection parameters are summarized in Table 2. Simulated particle positions are determined by the location of the parent body; the ejection velocities are uniformly distributed across the range of observed speeds of 0.2–1 m s⁻¹; and particle sizes are constrained to match the size distribution observed by the OSIRIS-REx mission science team. We do not try to simulate potential observational biases in particle size or ejection direction (Chesley et al., 2020). Figure 2 shows our simulated particle size distribution, with particles ranging from 0.1 to 2.5 cm in diameter and grouped into 24 bins. These particle sizes directly determine the β of each simulated particle, assuming a particle density of 2,000 kg m⁻³ (Equation 1).

Bennu produces on the order of 10⁴ g of material per orbit with 30% of that mass on hyperbolic trajectories (Hergenrother, Maleszewski, et al., 2020). Converting Bennu's orbital mass loss to annual mass loss (365 days per year/438 days per orbit), the hyperbolic ejecta amounts to 2,500 g per year. Our software is set up to introduce new particles at a constant, weekly, cadence. To account for the 2,500 g of new material entering the simulation per year, we use a production rate of 95 particles per week.

The integration of many thousands of particles is a computationally expensive task. Even running the simulation at one ejection per week produces tens of thousands of particles on orbits close to Bennu's orbit, where stream members experience close encounters with Earth on an annual basis. This requires the integrator to use very small step size increments to maintain accuracy.

Because we assume that the particles do not interact with each other, our solution was to break the 355 years (1780–2135) of particle production in each simulation down into 3-year groups, or “chunks.” Each chunk covers 3 years of 1 particle per week production and represents an average of 157 particles. These particles all experienced identical representations of the solar system between the years 1780 and 2200 and were able to be simulated on a single machine in about a quarter of the time that would otherwise have been required. To achieve a particle production rate of 95 particles per week, we simply restart the process 95 times. This is parallelized between multiple processors which enabled the simulation of 1,764,625 unique particles. These sum to a total mass of 2,056 kg introduced and simulated in the particle stream. Comparing this mass to the production rate reported by Hergenrother, Maleszewski, et al. (2020) of 2.5 kg/year \times 355 years = 888 kg, we consider our results optimistically representative of Bennu mass loss for this time frame.

Measurements of associability, stream elements, and encircling are made on the 3-year 157-particle sub-streams which are compiled together for final analysis. To collect data on the near-Earth particles, a sphere with radius equal to 300-Earth radii is centered at Earth. Any particle that enters that sphere is tracked until it reaches its minimum distance to Earth, where the heliocentric and geocentric state vectors are recorded for later use in impact and meteor-flux probability analysis. Figure 4 depicts the size scale of the data acquisition region. The particle stream in this example is a super-set of particle positions in 2135 as produced by our simulations. The year 2135 is chosen for Bennu's known close approach with Earth. Many young (age: 1–20 y.o.) particles are trailing behind Bennu while some older particles (age: 30–50 y.o.) are preceding Ben-

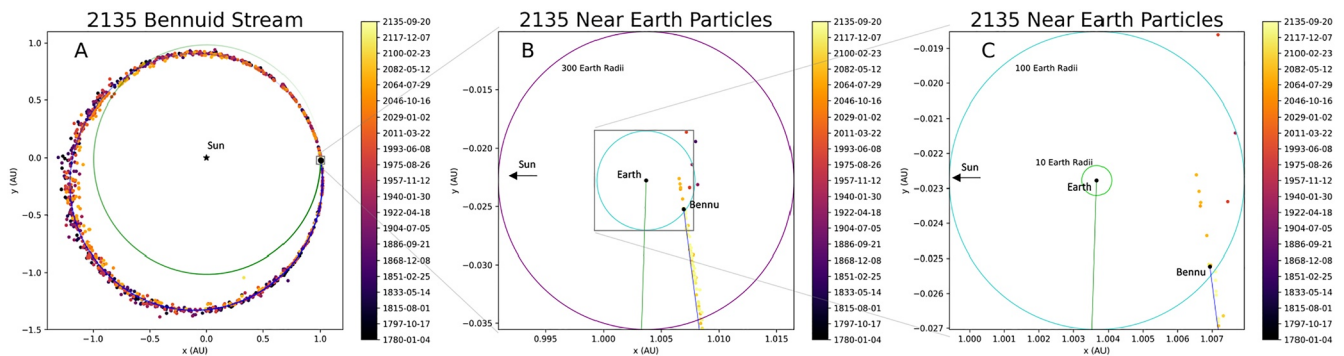


Figure 4. Panel (a) is a full view of a potential Bennuid particle stream in 2135 as Earth (orbit in green) nears the Earth-Bennu minimum orbital intersection distance (MOID). We collect data on all simulated particles within 300-Earth radii, as shown in panel (b). Panel (c) shows the location of the 10-Earth radius for context. Panels (b) and (c) also demonstrate that the youngest material (orange-yellow) tends to stay closely correlated to Benu's position (orbit in blue).

nu, experiencing even more significant Earth close approaches. Because Benu itself will not impact Earth over our time interval, we do not expect to observe flux from particles much younger than the timescale of encircling.

5. Data Analysis and Results

To provide context for the primary simulation, first, we address the relevance of SRP and PR through analysis of the timescale of encircling as described in Ye, Brown, and Pokorný (2016) and Ye et al. (2018). Throughout the simulation, the standard deviation of the particle streams' mean anomaly is calculated. The stream is said to be encircled if it reaches the encircling limit of $\sigma M \geq 60^\circ$, where σ is the standard deviation of the mean anomaly M . This limit is a fairly accurate metric of encircling as 3σ gives a range of $\pm 180^\circ$ and is representative of 99.7% of the stream members (Ye, Brown, & Pokorný, 2016; Ye et al., 2018). Second, we investigate the timescale of particle stream associability using the D_{sh} criterion. Meteoric activity observers have determined that bodies with $D_{sh} \leq 0.15$ can be correctly associated with the parent body (Jenniskens, 2006). At regular intervals, we compare all particle stream members to the current orbit of their parent body. These results are relative to a start date for particle production of 1780 though there is reason to suspect that particle production has been part of Benu's history before this (Hergenrother, Adam, et al., 2020). In general, we will show how our simulation results compare with the initial investigations of Kováčová et al. (2020) and Ye (2019). What differs between their studies and ours is that we reduce assumptions about the particle production style and use a much higher number for total particle production, thus ultimately producing a more accurate estimate of meteor flux throughout the simulated period.

5.1. Timescale of Encircling

Our simulations produced nearly 1.8 million particles, each with distinct ejection velocities and sizes. Resulting from realistic differences in their initial conditions, these particles encircle Benu's orbit in 80 ± 40 years. The fastest substream encircled in 14 years. Figure 5 shows an example of stream encircling, comparing the approximated constant production rate (95 particles/week in the model) to single-event production. Both streams begin to encircle around the same time, prompted by near-Earth approaches in 2054 and 2060 which are marked by vertical dashed lines. Constant particle production by the parent body results in a stream encircling faster than particles released in a single event. Panels (a)–(d) of this figure provides a visualization of meteoroid stream encircling. Panel (d) corroborates previous assertions that particles will be near Earth, each mid-September, as the stream becomes encircled.

Our modeled encircled particle stream resulted in the presence of particles within Earth's Hill Sphere every year after 1966, 186 years after the model begins. The very first particle to pass this close to Earth did so in 1896, long before Benu's first close-approach within this region in 2060. This particle stream's progress toward encircling is heavily driven by close approaches. Particles will remain relatively close to Benu with only ejection velocities and radiation forces to drive differences between them and their parent body. As a

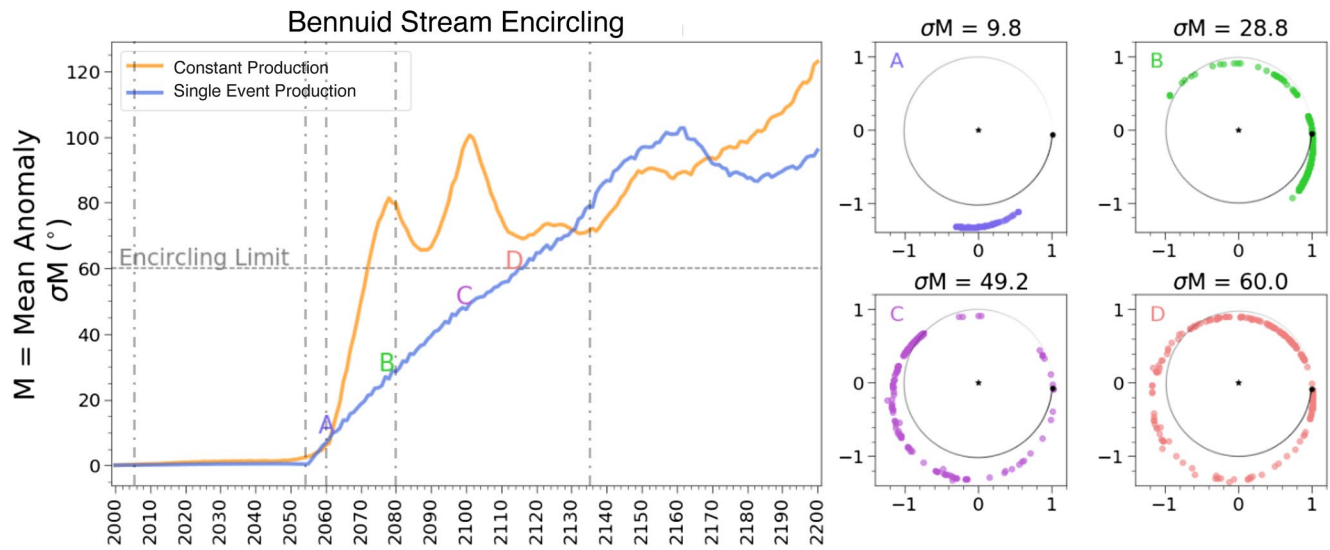


Figure 5. Time evolution of σM (left panel) with visual examples of particle spread at various levels of encircling (right panels). This figure compares the time for encircling from a single event (blue curve) with that of the constant particle production case (yellow curve).

result, the substreams which took the longest to encircle were all produced within the dynamically calmest period of 1850–2000.

5.2. Particle Associability

Figure 6 shows that 99.33% of our stream of 1.8 million particles remains associable to Bennu for the entirety of the simulated time range 1780–2200. Bennu’s close approaches are noted in the vertical dashed lines, the effect of which can be best observed during the 1788 and 1848 approaches which are correlated with an increasing spread of the populations D_{sh} values. The 0.67% that dissociate from Bennu are caused by very close encounters with Earth that result in highly perturbed trajectories such that their orbits are no longer comparable to Bennu’s. Even these perturbed particles remain associable with Bennu for the first 320 years of the simulation. This means that there is a good chance that a successful observation of these meteors would be recognized as coming from Bennu.

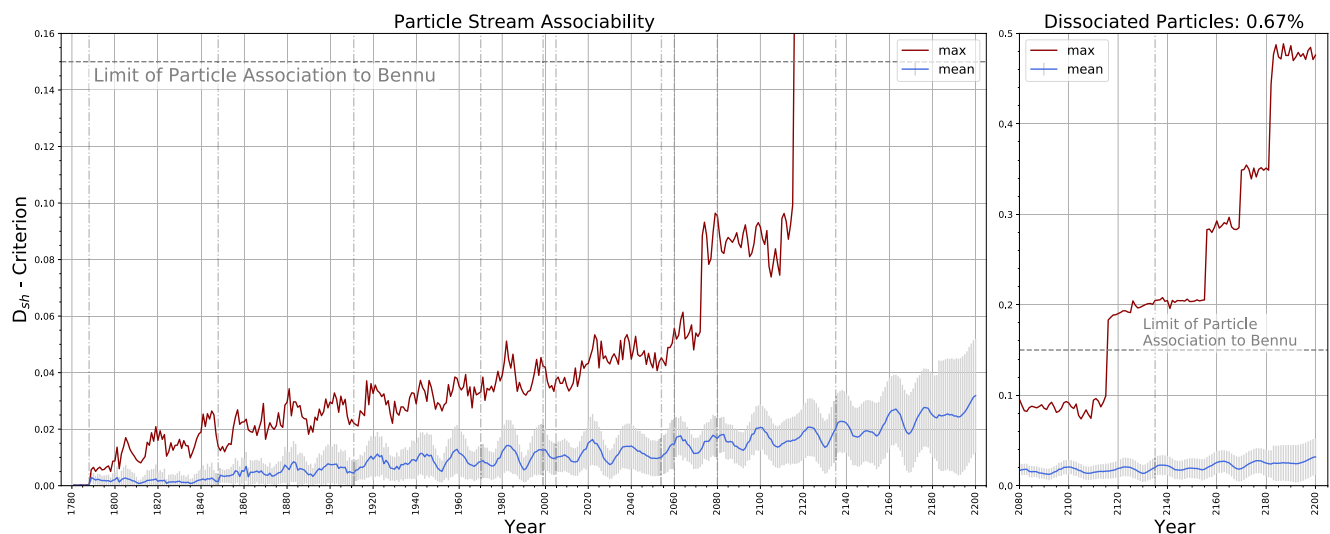


Figure 6. Particles ejected from Bennu remain associable for at least 150 years according to our calculation of the D_{sh} criterion as defined by Southworth and Hawkins (1963). Only 0.67% of particles are predicted to lose their association to Bennu by 2200.

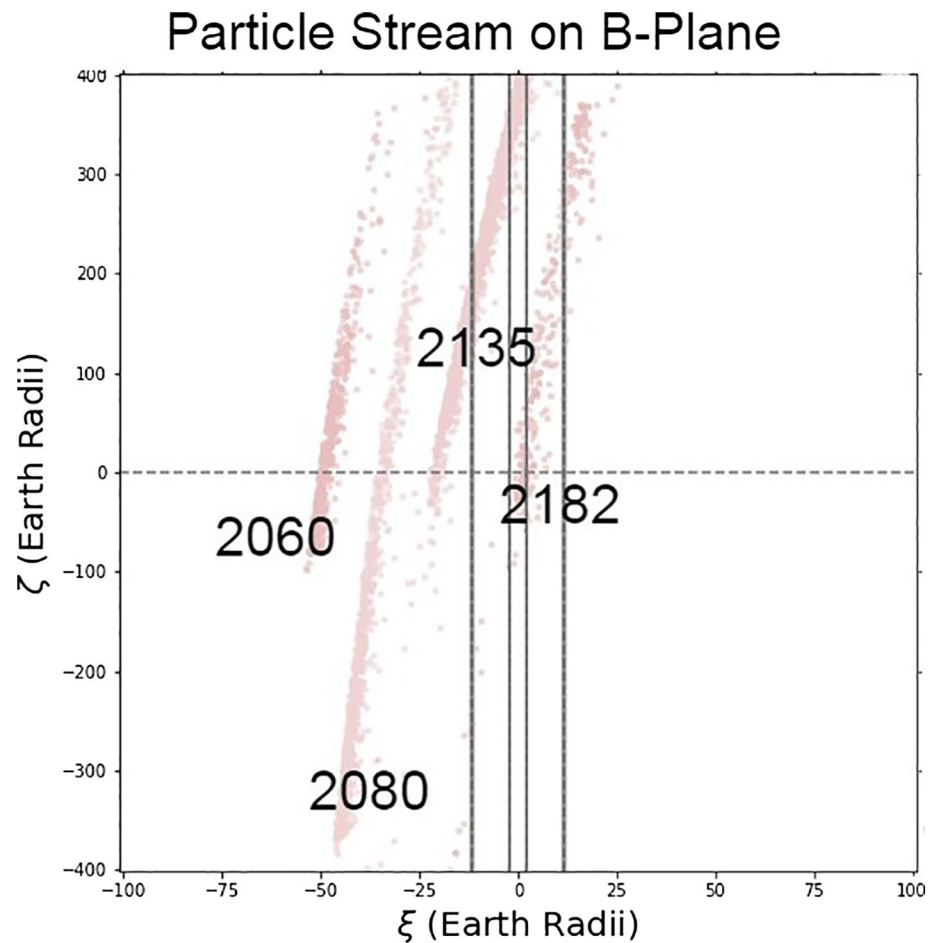


Figure 7. A particle stream from 2050 to 2135 (years chosen for computational convenience) is observed to evolve continuously toward a high meteor flux encounter in 2182. The stream is plotted on the B-plane in the Öpik framework. The mirrored vertical lines show the ± 10 -Earth radii (thicker lines) and ± 2.5 Earth radii (thinner lines) regions.

5.3. Analysis of Impactor Flux at Earth

B-plane analysis is a method used in large-body impact hazard prediction (Chesley et al., 2014; Farnocchia et al., 2019; Valsecchi et al., 2003). By saving the states of particles within Earth's Hill Sphere, the region around Earth where its gravity dominates, we can reduce the particle's interaction with Earth to the two-body problem. Once a particle is close to Earth, we can change to a geocentric reference frame in which the particle will appear to be on a hyperbolic orbit about Earth. The B-plane is defined as the plane that is both passing through the origin of Earth and normal to the asymptotic inbound velocity of each particle, hereby denoted as v_∞ . A vector B is then projected from Earth's origin to the point where the particle will intersect the plane. Impact is defined as whether the magnitude $B = |\vec{B}|$ is less than Earth's capture distance, which is ~ 2.5 Earth radii for this system.

The two-body approach formulation can be analyzed by transforming the Öpik reference frame (ξ, ζ) onto the B-plane such that $-\zeta$ is oriented with the projection of the heliocentric velocity of the planet and ξ can be taken as the MOID. We can obtain information on the MOID ($|\xi|$) and relative timing ($|\zeta|$) of each particle's near-Earth approach. For particle impacts from Bennu, Earth needs to pass through a coherent portion of the meteoroid stream. Figure 7 plots the particle stream on the B-plane, providing perspective on the timing and positions of our stream over time. The MOID of the meteoroid stream decreases toward zero until 2182, where a portion of the stream is shown to overlap with Earth (at the origin) at the right time and place for numerous impacts. These impacts are analyzed below in Section 5.3.2.

Table 3
Annual Bennuid Meteor Flux Rates at Earth

Peak time UT (Y-M-D hh:mm)	Duration (hh:mm)	Peak hourly Impactors
2125-09-25 01:15	04:50	1
2127-09-25 18:02	03:42	1
2129-09-25 05:02	03:12	2
2130-09-25 08:22	03:40	1
2133-09-25 00:18	07:45	2
2134-09-25 11:15	00:24	2
2135-09-25 12:29	11:53	2
2136-09-25 01:16	03:06	2
2137-09-25 11:00	00:31	2
2138-09-25 09:54	02:13	1
2139-09-25 12:52	08:31	1
2140-09-24 23:40	02:59	2
2141-09-25 06:57	04:02	2
2142-09-25 09:46	03:51	3
2143-09-25 12:09	10:01	2
2144-09-24 21:19	08:11	2
2145-09-24 23:09	06:29	1
2146-09-25 04:55	10:26	1
2147-09-25 12:04	09:09	2
2148-09-24 19:36	12:02	1
2150-09-25 03:13	05:23	1
2151-09-25 13:58	04:15	3
2152-09-24 17:32	08:03	2
2153-09-25 00:37	07:45	4
2154-09-25 05:52	00:19	5
2155-09-25 16:25	06:33	2
2156-09-24 18:18	06:52	3
2157-09-25 00:06	05:18	2
2158-09-25 05:38	06:32	2
2159-09-25 10:39	09:36	4
2160-09-24 12:43	09:13	2
2161-09-24 22:01	06:04	2
2162-09-25 00:42	10:06	2
2163-09-25 09:43	06:53	2
2164-09-24 14:55	06:20	3
2165-09-24 23:53	04:38	2
2166-09-25 03:31	05:29	3
2167-09-25 04:50	03:24	2
2168-09-24 16:56	05:37	2
2169-09-24 22:59	04:32	14
2170-09-25 03:23	04:18	3

Though we initially thought to consider particles within 10-Earth radii as potential impactors, such an assumption would require the particle stream to be of near uniform density across this region. Figure 7 refutes this assumption as the particle streams projected on the B-plane exhibit stream widths < 5 Earth radii. Figure 4c presents another view of this region. Therefore, rather than defining very close particles as impactors, we implemented a search in our integrations for hard-sphere particle collisions. Table 3 details the predicted meteor flux through the provision of the maximum particle impacts in an hour. The predicted duration is derived from the 1σ spread in recorded impact times. As expected, these annual flux estimates indicate that the results of Ye (2019) are an overestimate, possibly due to their use of an upper limit on mass loss predicted using the high uncertainty Spitzer data (Emery et al., 2014). Figure 8 shows the number of particles that impact Earth and Moon throughout the simulations. These “true impacts,” and their initial conditions are analyzed in the following section. We find that the year 2182 has the most impactors with 161 counted within a 3-h period. Analysis of the 2182 storm is continued in Section 5.3.2. We will show that this peak is not a sampling error but is, in fact, an example of a best-case scenario of Earth crossing through the densest portion of our particle stream.

5.3.1. Analysis of Impactors

Of the ~1.8 million particles produced during our simulated period of particle production (1780–2135), 676 particles impact Earth and 6 impact the Moon. The distribution of impacts per year is shown in Figure 8. Our model finds the first impact to be at the Moon in 2071 (291 years after start), with the first at Earth occurring in 2101 (321 years after start). The rates of these impact numbers steadily increase until the September 2182 storm which accounts for >23% of our models recorded impactor flux.

Bennu close approach years do not appear to correlate with impactor counts. Comparing the size distribution of these particles to the size distribution of all simulated particles shows no bias (Figure 9). The total stream population was produced with initial velocities that were evenly distributed between 0.2 and 1.0 m/s, and the impacting particles still maintain that trend, as shown in Figure 10. Our particles were introduced in weekly intervals about Bennu’s orbit which results in an even distribution of the particles’ initial Keplerian mean-anomaly. Figure 11 shows that impacting particles from all years except those involved in the 2182 storm are evenly distributed in mean anomaly.

5.3.2. Analysis of the 2182 Bennuid “Storm”

The year 2182 recorded five times more impacting particles than any other single year. We examined this result to ensure that it was not a sampling error or otherwise biased result. The distribution of particle ages at impact, shown in Figure 12, shows that these impacting particles are produced over a range of 66 years. Figure 13 adds to our understanding by showing a comparison of ejection years and particle size. If our 2182 storm were the result of a sampling bias, such that nearly all 161 impactors were born during the same 1 or 2 weeks, these two plots would have shown peaks centered at one or two years. By considering our result shown in Figure 7 that Bennu’s particle stream is crossing Earth’s path and the peak impact rate of 137 particles per hour as reported in Table 3,

Table 3
Continued

Peak time UT (Y-M-D hh:mm)	Duration (hh:mm)	Peak hourly Impactors
2171-09-25 07:43	04:48	2
2172-09-24 14:33	05:25	2
2174-09-25 02:15	04:54	4
2175-09-25 04:46	09:25	2
2176-09-24 09:33	07:52	1
2177-09-24 19:47	06:53	1
2178-09-25 03:48	07:12	4
2179-09-25 03:55	05:13	5
2180-09-24 13:11	05:53	4
2181-09-24 15:46	02:52	8
2182-09-24 23:04	03:17	137
2183-09-25 16:07	11:11	3
2184-09-24 09:18	07:18	2
2185-09-24 14:31	05:05	4
2186-09-25 01:21	04:44	3
2187-09-25 07:08	06:03	3
2188-09-24 06:46	09:55	2
2189-09-24 15:07	04:36	4
2190-09-25 02:33	04:36	10
2191-09-25 04:35	01:28	1
2192-09-24 07:59	09:58	1
2193-09-24 15:17	11:32	7
2194-09-24 19:00	05:58	3
2195-09-25 02:00	05:35	13
2196-09-24 08:26	02:08	22
2197-09-24 15:06	04:06	1
2198-09-24 14:41	08:32	1
2199-09-25 01:01	10:50	4

we see that 2182 is an ideal year for a major intersection between Earth and Bennu's meteoroid stream (a Bennuid storm).

The age breakdown (Figure 12) shows that most of the impacting particles were produced over a 60-year period between 2085 and 2125. The close encounter breakdown in Figure 1 shows that the time range, 2080–2135, is a dynamically calm period, so we expect that many of the particles produced during this time range stay within a half revolution from Bennu. The (b) panels of Figures 9–11 are reproduced in more detail in Figure 14. Figure 14c shows that, unlike the rest of impacting particles, the 2182 impactors were produced within a defined range of mean anomalies, which ranges from approximately one third of Bennu's orbit centered at a mean anomaly of 315° to just before perihelion, where Bennu is closest to Earth.

So, we have a specific group of particles produced during a calm period of time in a well-defined region of Bennu's orbit. Figures 14a and 14b show that there is no bias in speed or size. What then is the reason behind this storm in 2182? We find our answer in a study by Chesley et al. (2014) on Bennu's impact probabilities between 2175 and 2200 as a result of keyholes (temporally correlated positions around a massive body that ensure future impacts upon entry), produced by Bennu's close encounter with Earth in 2135. We analyzed these 161 particles for a close approach with Earth in 2135 and found that 150 particles, split between two groups, were present.

Analysis of 11 particles not near Earth in 2135 shows them to be characteristically similar to impactors of other years. We have labeled these 11 particles as "interlopers" and consider them to be background Bennuids.

The remaining 150 particles are plotted on the B-plane in 2135 in the first panel of Figure 15, which includes age and relative size. This figure shows that two dynamically distinct streams experience Earth encounters in 2135 which set up different resonant returns to Earth in 2182. The smaller group, Group 1, of only 12 particles makes an intermediary Earth approach in 2155 resulting in a 27:23 resonance with Earth. The larger group, Group 2, makes an intermediary close approach in 2162 resulting in a 20:17 resonance to Earth. The particles of Group 2 were produced over a range of 60 years with varying sizes and speeds, but their orbital position during ejection selects these particles to impact Earth in 2182 when the meteoroid stream's MOID is zero. With these 150 particles impacting within 1 h and 40 min, this "storm" is representative of the best conditions for particle flux at Earth from Bennu.

The occurrence of particles entering this dynamical path to impact in 2182 is affirmation that long-term particle production is necessary to best predict the future of non-cometary meteoroid streams. It is possible that Kováčová et al. (2020) missed finding the 2182 storm because their simulation included particle production only during one initial Bennu orbit. In contrast, our simulation of continuous weekly production throughout the duration of the time period has allowed the ejected Bennuids to reveal the unique initial conditions that led to this otherwise overlooked keyhole.

6. Conclusions

We used a precision historical solar system integrator (REBOUND), parameterized on the basis of OSIRIS-REx observations of particle ejection from asteroid Bennu, to predict the flux of Bennuid meteors to Earth. These simulations show that discrete weekly particle ejection events (95 particles/week) allow for

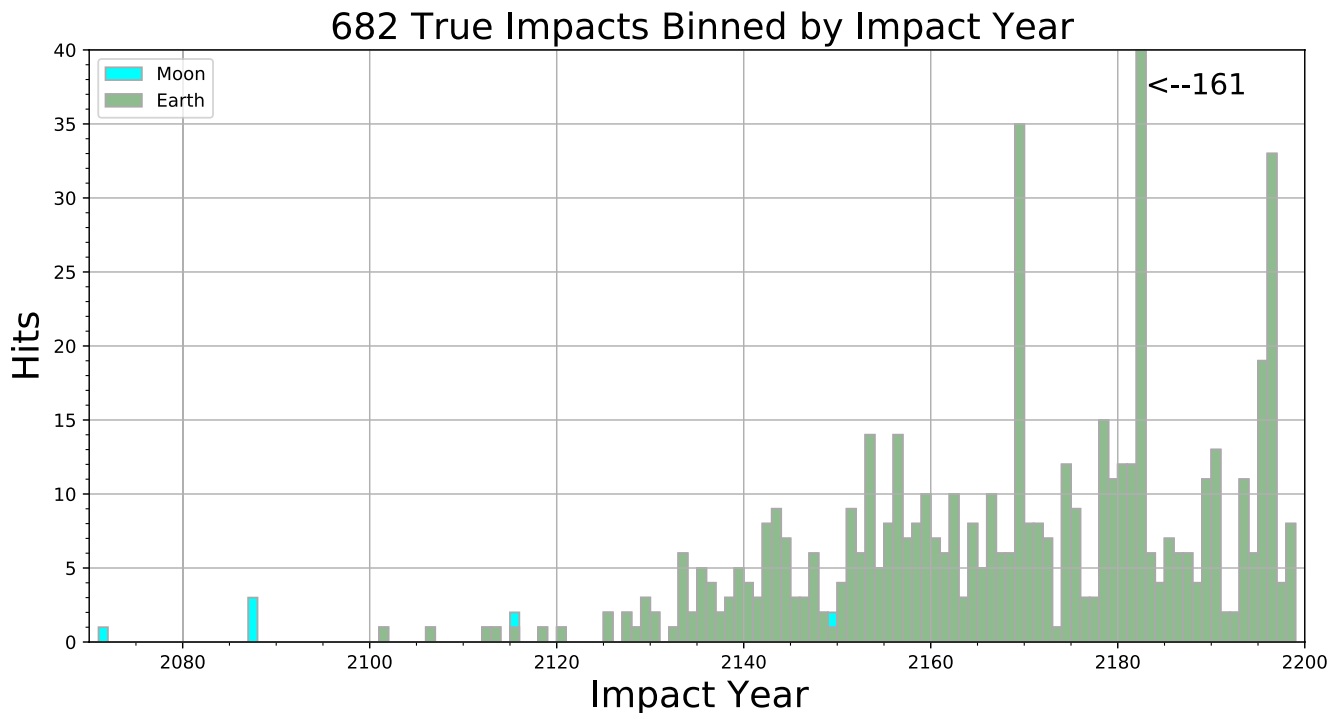


Figure 8. Recorded impact distribution at Moon (blue) and Earth (green) for each year of our simulation. The vertical axis is truncated for reasonable scaling of the majority of years.

encircling of the particle stream within 80 years after ejection. Individual particles (and the stream) remain associable to Bennu for the entire simulation timescale of 420 years.

This simulation confirms that material ejected from Bennu will intersect with Earth in the future and likely already has. We predict that particle flux rates at Earth will be extremely low, much less than a particle per year until near 2101 as the Bennu-Earth MOID reaches values less than Earth's cross section of impact. Our simulated highest particle flux in 2182 converts to a zenith hourly rate (ZHR) of > 0.1 or one meteor observed in 10 h. This is comparable to the lowest recognized flux from known showers. Major showers like the Geminids dwarf this rate by three orders of magnitude with a ZHR > 100 year to year (Jenniskens, 2006).

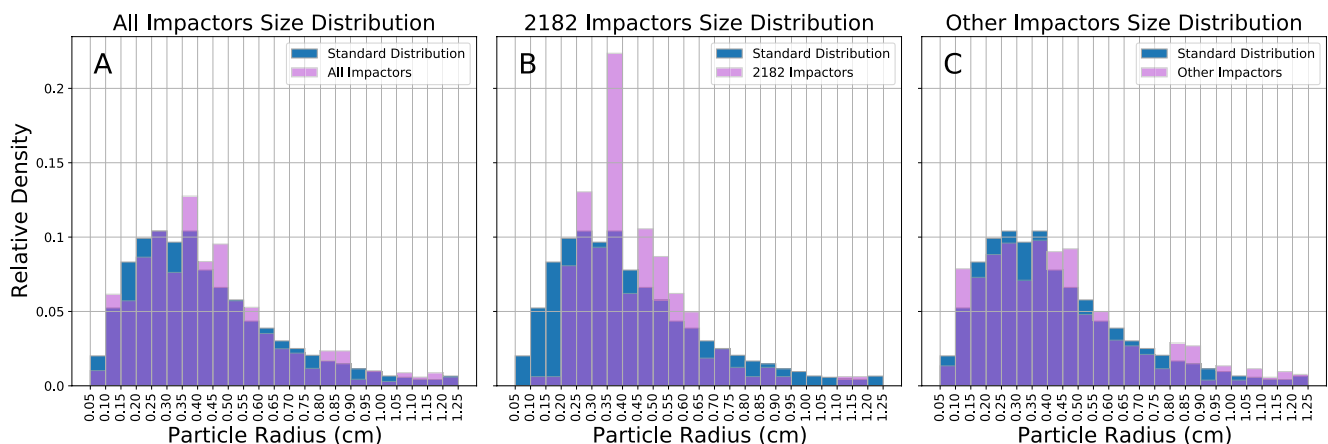


Figure 9. Size distribution of simulated particles intersecting Earth compared to the expected size distribution. Panel (a) compares all 682 impactors. Panel (b) compares only the 2182 impactors. Panel (c) shows the distribution without the 2182 impactors.

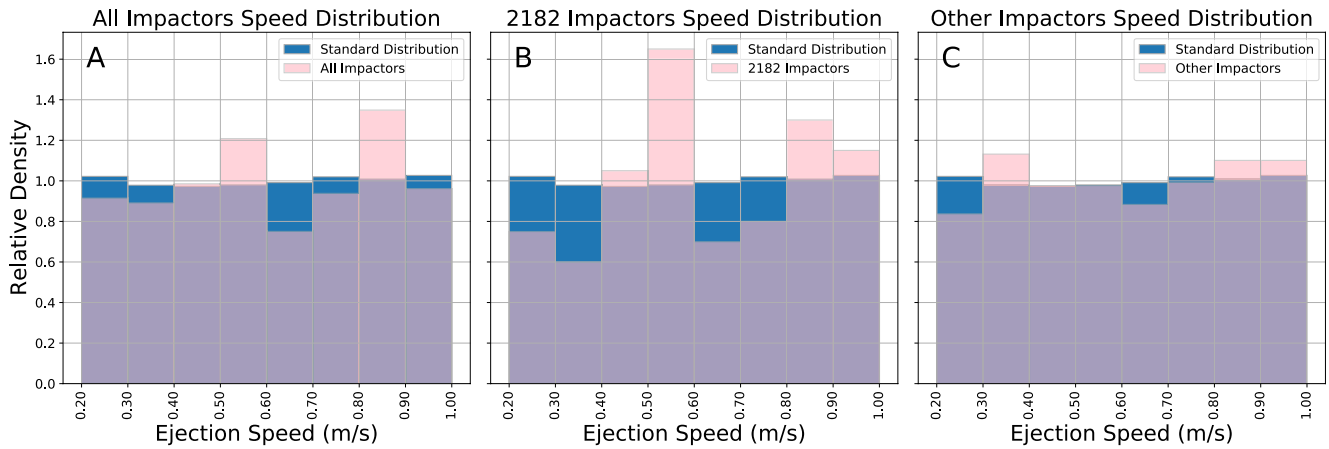


Figure 10. Speed distribution of particles intersecting Earth following same format as Figure 9.

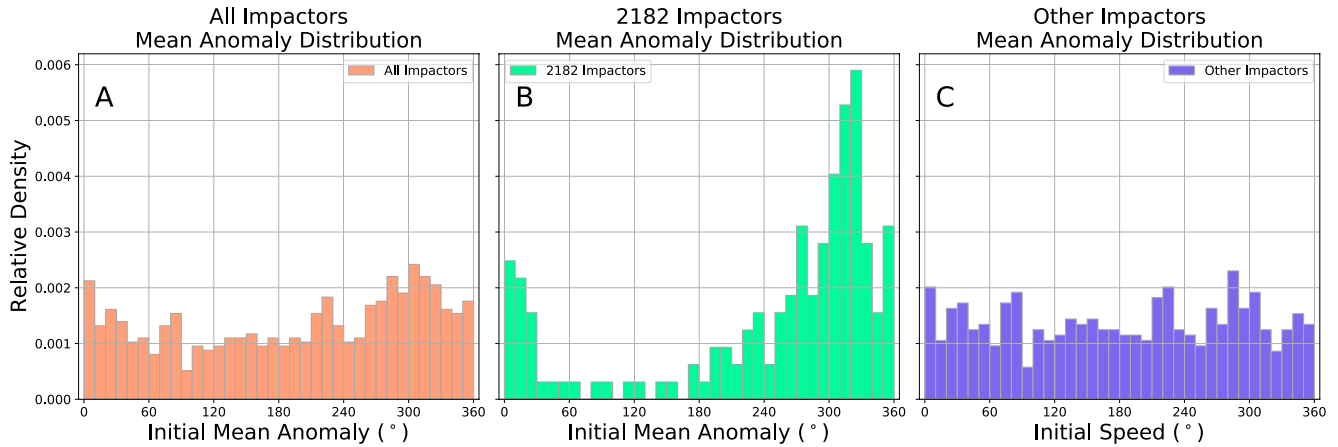


Figure 11. Distribution of initial mean anomaly at ejection for particles intersecting Earth. Panel (a) shows all 682 impactors. Panel (b) shows the 2182 impactors. Panel (c) shows the distribution without the 2182 impactors.

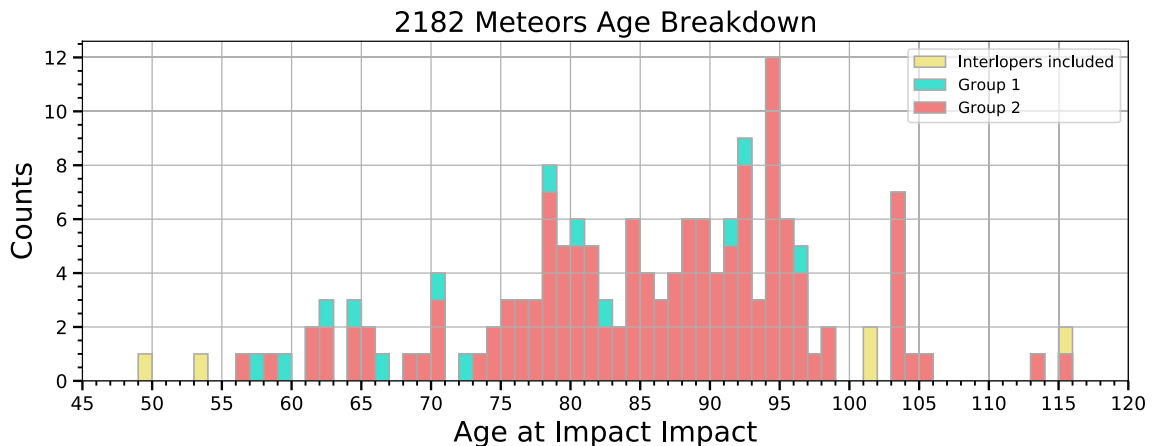


Figure 12. Two separate particle streams are responsible for the meteors predicted to intersect Earth in 2182. The 12 members labeled Group 1 are shown in blue. The 138 members labeled Group 2 are shown in red. The average age of these particles matches the expected timescale of encircling.

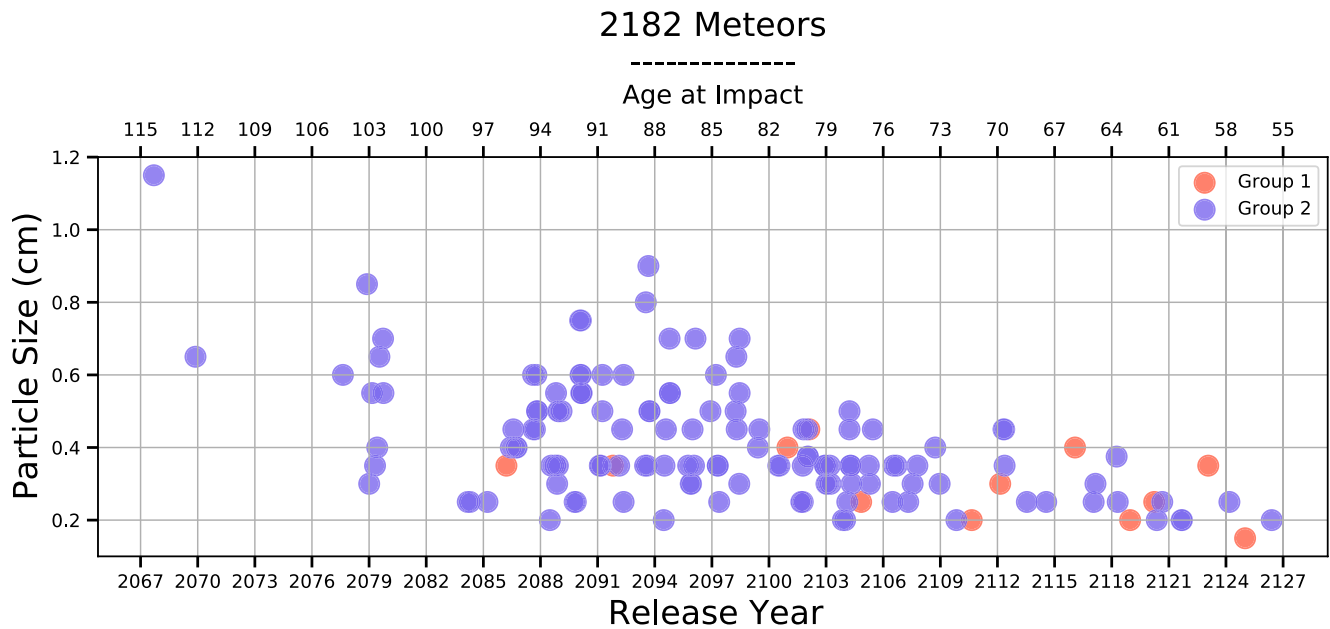


Figure 13. Relationship between particle age and particle size for the two coherent streams which contribute to the 2182 meteor shower.

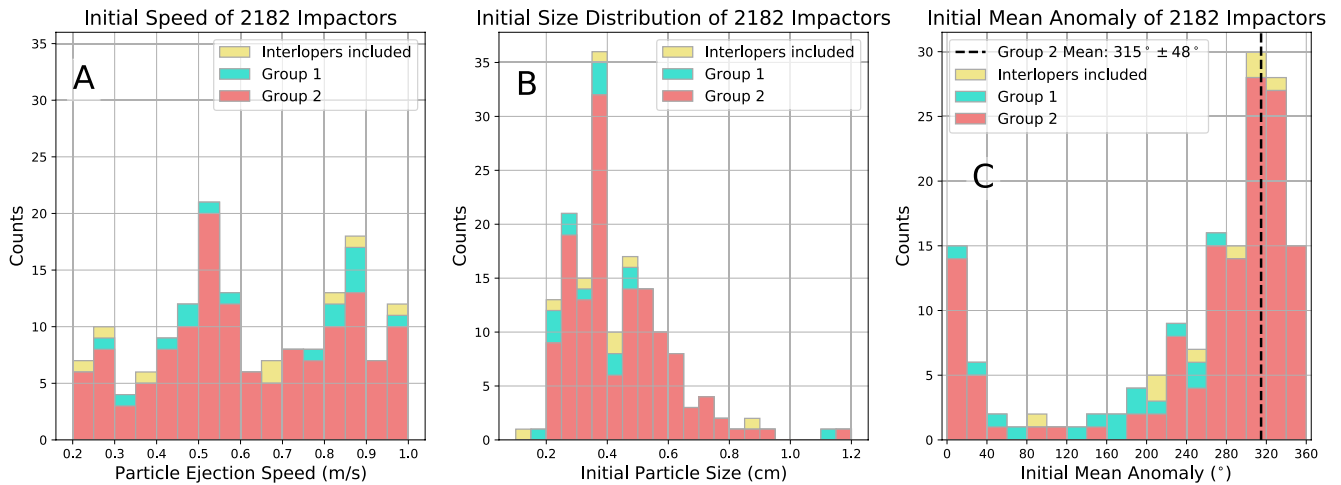


Figure 14. The predicted 161 2182 impactors can be categorized by their orbital route to impact. Panel (a) shows the ejection speed distribution, colored by group, panel (b) shows each group's size distribution, and panel (c) shows the groups' distributions of initial mean anomaly, or the mean anomaly of each impacting particle at their time of birth.

We expect that the 3-h window offered by the 2182 storm is the only reasonable chance to observe meteors from Bennu.

Due to the uncertainties in Bennu's long-term position that constrained our particle propagation time period, these results are a lower bound on Bennuid flux rates. A followup investigation of potential pre-1780 initial conditions may allow for the propagation of an older meteor stream and lead to additional flux.

In our study, the increase in flux rates were not correlated with close approaches of the parent body Bennu, but we observe that the densest portion of the meteoroid stream remains near the parent body. This finding suggests that more significant meteoric activity is possible from near-Earth asteroids that pass closer to Earth than does Bennu. Asteroid (99942) Apophis is an ideal candidate for such activity at Earth with a close approach distance of 37,700 km (5.9 Earth radii) in 2029.

150 Particles from Bennu Showering onto Earth in 2182

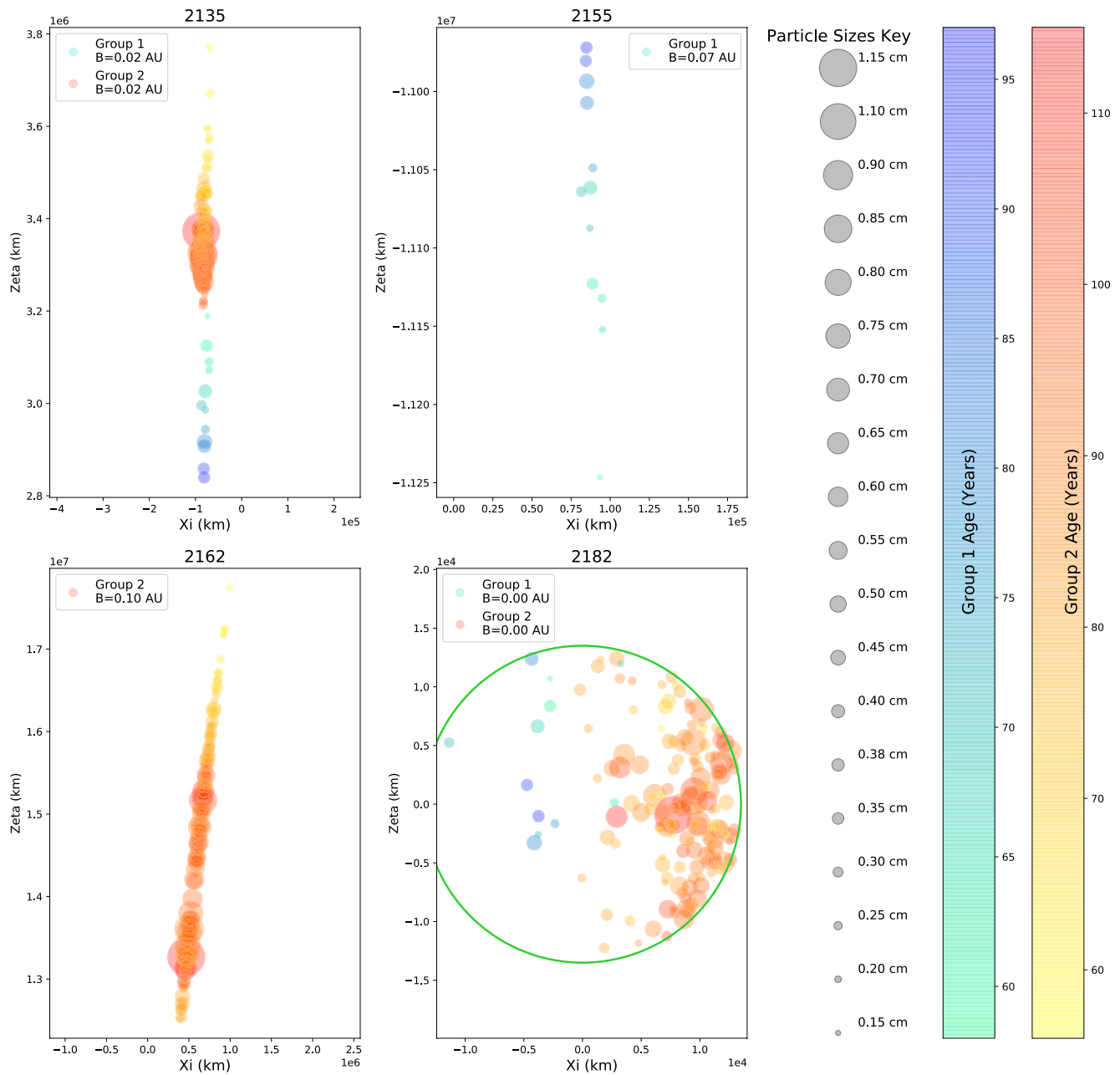


Figure 15. Of the 161 particles which impact Earth in 2182, 150 can be dynamically linked to an Earth approach in 2135 which determines their path toward impact. Particle sizes and ages are represented according to the keys available in the figure. Group 1 is represented in gradients of blue while Group 2 is in gradients of red based on particle age at impact. Group 1's intermediary close approach in 2155 is shown along with Group 2's intermediary close approach in 2162. Group 2 is shown to have a tight impact cluster along the right limb of Earth.

The process that is leading to mass loss on Bennu is probably not unique to Bennu (Hergenrother, Adam, et al., 2020). Thus, the discovery of particle ejection from Bennu opens up an avenue of investigation into meteors originating from the near-Earth asteroid population. The methods presented here can be expanded upon to give us insight into the history and structure of what is now regarded to be the “background” meteoroid population.

Developments in the field of dynamically tracking debris in space may be of interest to sectors other than astronomers. Improvements in our models of near-Earth asteroid ejecta could also be used to constrain safety margins for future missions to other bodies. Ejecta long-term evolution could be important to estimates of safety and expected lifetime for any near-Earth satellite.

Data Availability Statement

All parameters needed to reproduce our results are described in the text. Solar system ephemerides can be obtained from https://naif.jpl.nasa.gov/pub/naif/generic_kernels/spk/planets/ and the small bodies can be queried from JPL's Horizons interface Giorgini et al. (1996) and JPL Solar System Dynamics Group, NASA/JPL Horizons, On-Line Ephemeris System, <http://ssd.jpl.nasa.gov/?horizons>, data retrieved 2020-OCT-27. The raw numbers supporting all figures and tables in the text can be obtained at <http://dx.doi.org/10.17632/zn5bj55kgh.1> (Melikyan, 2020). Our model was developed with the REBOUND and REBOUNDx Python APIs (Rein & Liu, 2012; Tamayo et al., 2020).

Acknowledgments

This material is based upon work supported by NASA under Contract NNM10AA11C issued through the New Frontiers Program. The work of SRC was conducted at the Jet Propulsion Laboratory, California Institute of Technology under a contract with the National Aeronautics and Space Administration. The authors give special thanks to A. Ferro and C. Wolner who, respectively, provided the computational resources and manuscript preparation assistance necessary to complete this work. The authors are grateful to the entire OSIRIS-REX team for making the encounter with Bennu possible.

References

- Bos, B. J., Nelson, D. S., Pelgrift, J. Y., Liounis, A. J., Doelling, D., Norman, C. D., et al. (2020). In-flight calibration and performance of the OSIRIS-REX Touch And Go camera system (TAGCAMS). *Space Science Reviews*, 216(4), 71. <https://doi.org/10.1007/s11214-020-00682-x>
- Botke, W. F., Moorhead, A. V., Connolly, H. C., Jr, Hergenrother, C. W., Molaro, J. L., Michel, P., et al. (2020). Meteoroid impacts as a source of Bennu's particle ejection events. *Journal of Geophysical Research: Planets*, 125, e2019JE006282. <https://doi.org/10.1029/2019JE006282>
- Burns, J. A., Lamy, P. L., & Soter, S. (1979). Radiation forces on small particles in the solar system. *Icarus*, 40(1), 1–48. [https://doi.org/10.1016/0019-1035\(79\)90050-2](https://doi.org/10.1016/0019-1035(79)90050-2)
- Chesley, S. R., Farnocchia, D., Nolan, M. C., Vokrouhlický, D., Chodas, P. W., Milani, A., et al. (2014). Orbit and bulk density of the OSIRIS-REX target asteroid (101955) Bennu. *Icarus*, 235, 5–22. <https://doi.org/10.1016/j.icarus.2014.02.020>
- Chesley, S. R., French, A. S., Davis, A. B., Jacobson, R. A., Brozović, M., Farnocchia, D., et al. (2020). Trajectory estimation for particles observed in the vicinity of (101955) Bennu. *Journal of Geophysical Research: Planets*, 125, e2019JE006363. <https://doi.org/10.1029/2019JE006363>
- Emery, J., Fernández, Y., Kelley, M., Warden, K., Hergenrother, C., Lauretta, D., et al. (2014). Thermal infrared observations and thermo-physical characterization of OSIRIS-REX target asteroid (101955) Bennu. *Icarus*, 234, 17–35. <https://doi.org/10.1016/j.icarus.2014.02.005>
- Farnocchia, D., Eggl, S., Chodas, P. W., Giorgini, J. D., & Chesley, S. R. (2019). Planetary encounter analysis on the B-plane: A comprehensive formulation. *Celestial Mechanics and Dynamical Astronomy*, 131(8), 36. <https://doi.org/10.1007/s10569-019-9914-4>
- Folkner, W. M., Williams, J. G., Boggs, D. H., Park, R. S., & Kuchynka, P. (2014). The planetary and lunar ephemerides DE430 and DE431. *Interplanetary Network Progress Report*, 196(1).
- Giorgini, J. D., Yeomans, D. K., Chamberlin, A. B., Chodas, P. W., Jacobson, R. A., Keesey, M. S., et al. (1996). JPL's on-line solar system data service. In *AAS/Division for Planetary Sciences Meeting Abstracts #28* (pp. 25–04).
- Hamilton, V., Simon, A., Christensen, P., Reuter, D., Clark, B., Barucci, M., et al. (2019). Evidence for widespread hydrated minerals on asteroid (101955) Bennu. *Nature Astronomy*, 3(4), 332–340. <https://doi.org/10.1038/s41550-019-0722-2>
- Hergenrother, C. W., Adam, C. D., Chesley, S. R., & Lauretta, D. S. (2020). Introduction to the special issue: Exploration of the activity of asteroid (101955) Bennu. *Journal of Geophysical Research: Planets*, 125, e2020JE006549. <https://doi.org/10.1029/2020JE006549>
- Hergenrother, C. W., Maleszewski, C., Li, J.-Y., Pajola, M., Chesley, S. R., French, A. S., et al. (2020). Photometry of particles ejected from active asteroid (101955) Bennu. *Journal of Geophysical Research: Planets*, 125, e2020JE006381. <https://doi.org/10.1029/2020JE006381>
- Jenniskens, P. (2006). *Meteor showers and their parent comets*. Cambridge University Press.
- Kováčová, M., Nagy, R., Kornoš, L., & Tóth, J. (2020). 101955 Bennu and 162173 Ryugu: Dynamical modelling of ejected particles to the Earth. *Planetary and Space Science*, 104897.
- Lauretta, D. S., Hergenrother, C. W., Chesley, S. R., Leonard, J. M., Pelgrift, J. Y., Adam, C. D., et al. (2019). Episodes of particle ejection from the surface of the active asteroid (101955) Bennu. *Science*, 366(6470), eaay3544. <https://doi.org/10.1126/science.aay3544>
- Leonard, J. M., Adam, C. D., Pelgrift, J. Y., Lessac-Chenen, E. J., Nelson, D. S., Antreasian, P. G., et al. (2020). Initial orbit determination and event reconstruction from estimation of particle trajectories about (101955) Bennu. *Earth and Space Science*, 7, e2019EA000937. <https://doi.org/10.1029/2019EA000937>
- McMahon, J. W., Scheeres, D. J., Chesley, S. R., French, A., Brack, D., Farnocchia, D., et al. (2020). Dynamical evolution of simulated particles ejected from asteroid Bennu. *Journal of Geophysical Research: Planets*, 125(8), e2019JE006229. <https://doi.org/10.1029/2019je006229>
- Melikyan, R. E. (2020). Bennu's natural sample delivery mechanism: Estimating the flux of Bennuid meteors at earth. *Mendeley Data*. <https://doi.org/10.17632/zn5bj55kgh.1>
- Molaro, J. L., Hergenrother, C. W., Chesley, S., Hanna, R. D., Haberle, C. W., Ballouz, R.-L., et al. (2020). Thermal fatigue as a driving mechanism for activity on asteroid Bennu. *Journal of Geophysical Research: Planets*, 125, e06325. <https://doi.org/10.1029/2019JE006325>
- Rein, H., & Liu, S.-F. (2012). REBOUND: An open-source multi-purpose N-body code for collisional dynamics. *Astronomy & Astrophysics*, 537, A128. <https://doi.org/10.1051/0004-6361/201118085>
- Rein, H., & Spiegel, D. S. (2015). IAS15: A fast, adaptive, high-order integrator for gravitational dynamics, accurate to machine precision over a billion orbits. *Monthly Notices of the Royal Astronomical Society*, 446(2), 1424–1437. <https://doi.org/10.1093/mnras/stu2164>
- Southworth, R. B., & Hawkins, G. S. (1963). Statistics of meteor streams. *Smithsonian Contributions to Astrophysics*, 7, 261–285.
- Tamayo, D., Rein, H., Shi, P., & Hernandez, D. M. (2020). REBOUNDx: A library for adding conservative and dissipative forces to otherwise symplectic N-body integrations. *Monthly Notices of the Royal Astronomical Society*, 491(2), 2885–2901. <https://doi.org/10.1093/mnras/stz2870>
- Valsecchi, G. B., Milani, A., Gronchi, G. F., & Chesley, S. R. (2003). Resonant returns to close approaches: Analytical theory. *Astronomy & Astrophysics*, 408(3), 1179–1196. <https://doi.org/10.1051/0004-6361:20031039>

- Vaubailion, J., Colas, F., & Jorda, L. (2005). A new method to predict meteor showers-I. Description of the model. *Astronomy & Astrophysics*, 439(2), 751–760. <https://doi.org/10.1051/0004-6361:20041544>
- Weidenschilling, S. J., & Jackson, A. A. (1993). Orbital resonances and Poynting-Robertson drag. *Icarus*, 104(2), 244–254. <https://doi.org/10.1006/icar.1993.1099>
- Ye, Q.-Z. (2019). Prediction of meteor activities from (101955) Bennu. *Research Notes of the American Astronomical Society*, 3(3), 56. <https://doi.org/10.3847/2515-5172/ab12e7>
- Ye, Q.-Z., Brown, P. G., & Pokorný, P. (2016). Dormant comets among the near-Earth object population: A meteor-based survey. *Monthly Notices of the Royal Astronomical Society*, 462(4), 3511–3527. <https://doi.org/10.1093/mnras/stw1846>
- Ye, Q.-Z., Hui, M.-T., Brown, P. G., Campbell-Brown, M. D., Pokorný, P., Wiegert, P. A., & Gao, X. (2016). When comets get old: A synthesis of comet and meteor observations of the low activity comet 209P/LINEAR. *Icarus*, 264, 48–61. <https://doi.org/10.1016/j.icarus.2015.09.003>
- Ye, Q.-Z., Wiegert, P. A., & Hui, M.-T. (2018). In search of recent disruption of (3200) Phaethon: Model implication and Hubble Space Telescope search. *The Astrophysical Journal Letters*, 864(1), L9. <https://doi.org/10.3847/2041-8213/aada46>